Journal of ELECTRONIC MATERIALS, Vol. 42, No. 7, 2013
DOI: 10.1007/s11664-012-2438-2
© 2013 TMS

Fabrication by Coaxial-Type Vacuum Arc Evaporation Method and Characterization of Bismuth Telluride Thin Films

M. UCHINO,[1] K. KATO,[2] H. HAGINO,[1] and K. MIYAZAKI[1,3]

1.—Department of Mechanical and Control Engineering, Kyushu Institute of Technology, 1-1, Sensui-cho, Tobata-ku, Kitakyushu, Fukuoka 804-8850, Japan. 2.—Lintec Corporation, 5-14-42 Nishiki-cho, Warabi, Saitama 335-0005, Japan. 3.—e-mail: miyazaki@mech.kyutech.ac.jp

We prepared both *n*- and *p*-type bismuth telluride thin films by using a coaxial-type vacuum arc evaporation method. The atomic compositions of the as-grown thin films and several annealed thin films were comparable to that of bulk bismuth telluride. Their thermoelectric properties were measured and found to be comparable to those of bulk materials. The Seebeck coefficient and electrical conductivity of the as-grown thin films were improved by the annealing process. The measured figures of merit (*ZT*) of the films were 0.86 for the *n*-type and 0.41 for the *p*-type at 300 K for annealing temperatures of 573 K and 523 K, respectively.

Key words: Thermoelectricity, coaxial-type vacuum arc evaporation method, bismuth telluride, thin film

INTRODUCTION

Bismuth-telluride-based alloys are attractive thermoelectric materials. They are widely used in cooling devices and have been proposed for energy conversion applications at room temperature. The performance of a thermoelectric material depends on the dimensionless figure of merit, *ZT*, which is defined as $ZT = S^2\sigma T/\kappa$, where S is the Seebeck coefficient, σ is the electrical conductivity, κ is the thermal conductivity, and T is the absolute temperature. Recently, production of nanostructures in thermoelectric materials has been considered a promising way to improve *ZT* values by decreasing the thermal conductivity through enhanced phonon scattering at boundaries and interfaces while the electrical properties are maintained.[1–5] Mostly thin-film techniques have been used to make nanostructured thermoelectric materials.

There are many thin-film deposition methods, such as flash evaporation,[6–8] co-sputtering,[9,10] and metalorganic chemical vapor deposition (MOCVD).[11,12] Although many deposition methods have been developed, the resulting devices have not been commercially viable because of their high production costs (expensive equipment) or inadequate thin-film properties.[6] Here, we focus on a coaxial-type vacuum arc evaporation method.[13–15] This method is a kind of vacuum evaporation technique in which the cathode material is evaporated by arc discharge in vacuum. The atomic composition of the alloy is kept constant because of its high evaporation rate. The system for the coaxial-type vacuum arc evaporation method is very simple, with only a vacuum chamber, a target for the evaporation source, and a substrate holder. In this study, we prepared bismuth telluride thermoelectric thin films by the coaxial-type vacuum arc evaporation method. We investigated the effects of the annealing process on their thermoelectric properties (electrical conductivity, Seebeck coefficient, and grain morphology), because the thermoelectric properties of the as-grown films were very low. We discuss this coaxial-type vacuum arc evaporation method for the fabrication of bismuth telluride thin films with high *ZT* values.

(Received July 7, 2012; accepted December 28, 2012; published online February 21, 2013)

EXPERIMENTAL PROCEDURES

Both *n*- and *p*-type bismuth telluride thin films were fabricated on glass plates by the coaxial-type vacuum arc evaporation method followed by an annealing process. A schematic diagram of the

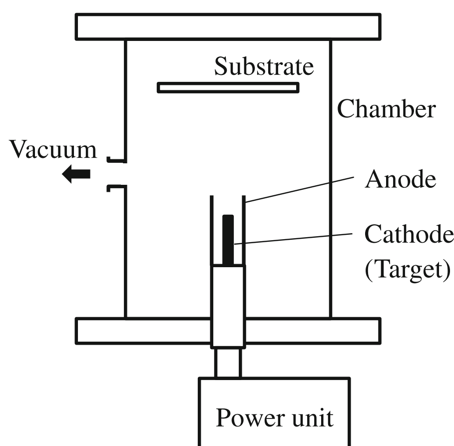

Fig. 1. Schematic diagram of coaxial-type vacuum arc evaporation equipment.

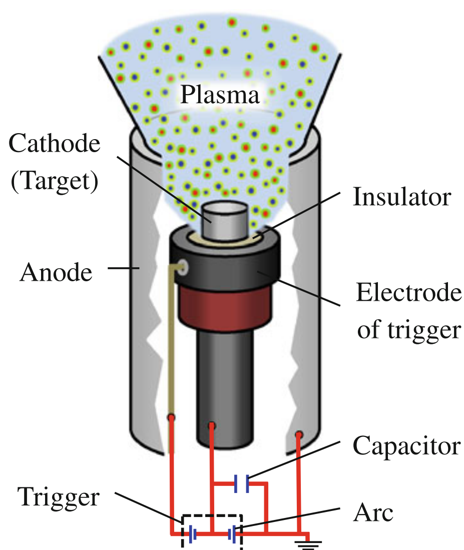

Fig. 2. Schematic diagram of coaxial-type vacuum arc evaporation source.

deposition equipment (ULVAC APG-1000) is shown in Fig. 1. The vacuum chamber contains a target for the evaporation source and a substrate holder. The distance between the target and substrate is 150 mm. Figure 2 shows a schematic diagram of the evaporation source. A high arc discharge current through the cathode (peak current exceeds 1000 A) induces a strong circumferential magnetic field. Ions and electrons moving radially in the arc discharge are accelerated toward the substrate by the Lorentz force and effectively collected on the substrate as shown in Fig. 2.[13] The chamber was evacuated to below 5.0×10^{-3} Pa by a turbomolecular pump. Then, the discharge voltage set to 80 V was applied 400 times at a frequency of 1 Hz. The

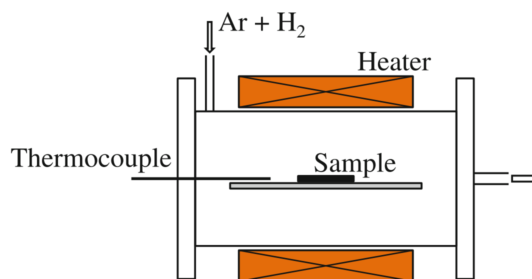

Fig. 3. Schematic diagram of annealing furnace.

deposition rates were 0.6 nm/s and 0.5 nm/s for the n-type and p-type films, respectively.

To investigate the effects of the annealing conditions on the thin-film properties, we chose one thin-film sample with uniform thickness and morphology, and cut it into small slices (25 mm length, 10 mm width). The cut samples were annealed in an electric furnace (φ92 mm, 550 mm length) (Fig. 3) with high-purity argon mixed with 5% hydrogen at 1.0 Pa for 60 min. We supplied the gas at a flow rate of 0.1 SLM during the sintering process. The sintering temperatures ranged from 473 K to 623 K. The temperature was increased at a rate of 5 K/min to the set temperature. The temperature in the furnace was measured by a thermocouple placed near the sample. After sintering, the furnace was cooled down naturally to room temperature. The crystal orientations of the thin films were evaluated by x-ray diffraction (XRD). The atomic compositions of the films were examined by energy-dispersive x-ray spectroscopy (EDS). The surface and cross-section morphologies of the thin films were investigated by means of scanning electron microscopy (SEM). The in-plane electrical conductivities of the thin films were measured at room temperature by a four-point probe method with accuracy of ±5%, and the in-plane Seebeck coefficients were measured at room temperature with accuracy of ±4%. One end of the thin film was connected to a heat sink and the other end to a heater. The Seebeck coefficient was determined as the ratio of the potential difference V along the film to the temperature difference T. The cross-plane thermal conductivity at room temperature was measured by a differential 3ω method with accuracy of 10%. Details of the thermal conductivity measurements have been described previously.[16–18] In brief, a SiO_2 film was deposited on the thin film. A thin aluminum wire was deposited on the sample through shadow masks. The aluminum wire was 20 μm wide, and the length of the heater was 2 mm. We fabricated reference samples that lacked the nanocrystalline thin film but were otherwise identical to the primary sample. The reference samples were used to subtract off the unknown thermal properties of the insulation layers. The figure of merit ZT was evaluated from the electrical conductivity, Seebeck coefficient, and thermal conductivity results.

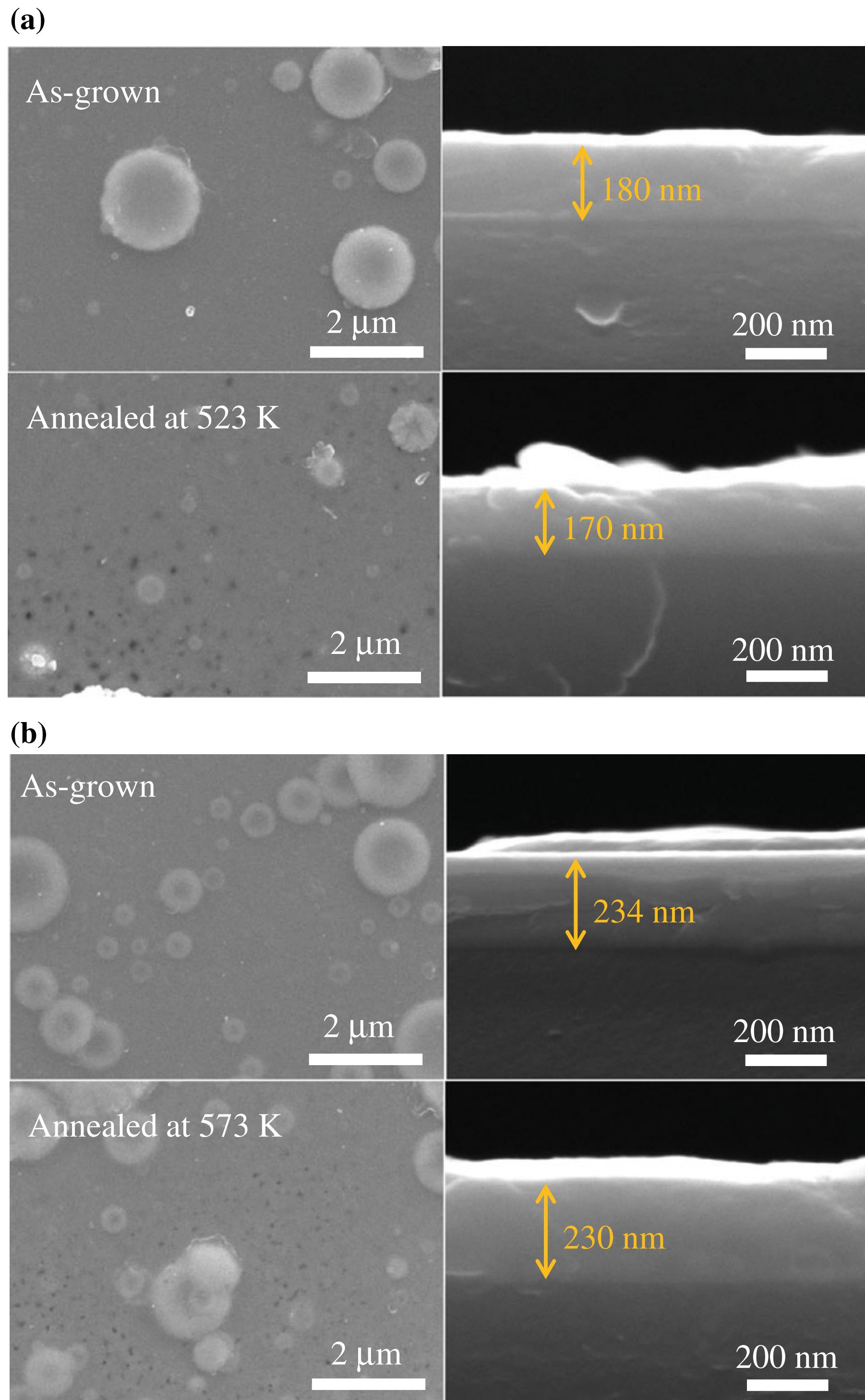

Fig. 4. (a) Surface and cross-section micrograph of as-grown and annealed at 573 K *n*-type bismuth telluride thin films. (b) Surface and cross-section micrograph of as-gown and annealed at 523 K *p*-type bismuth telluride thin films.

RESULTS AND DISCUSSION

The surface and cross-section morphologies of both as-grown and annealed bismuth telluride thin films were investigated by means of SEM (Fig. 4). Microparticles were observed on the films, although the thickness of the microparticles was about only 10 nm by SEM imaging. These particles were observed even after the annealing process. Nanometer-sized holes were observed on the surface of the annealed thin films. Deposited thin films had

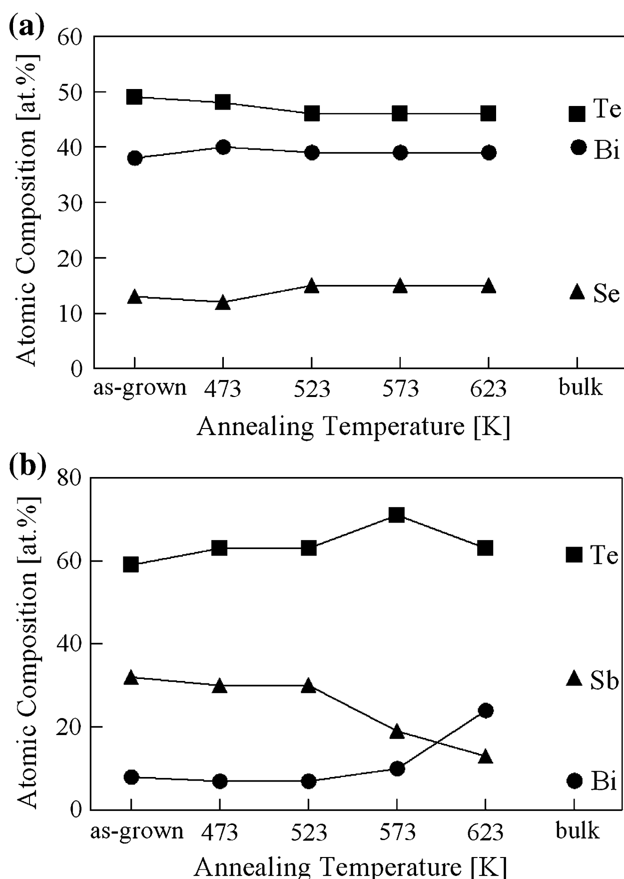

Fig. 5. (a) Atomic compositions of *n*-type bismuth telluride thin films. (b) Atomic compositions of *p*-type bismuth telluride thin films.

high density based on cross-section imaging, although some nanoholes were observed on the surface. Only materials on the surface were evaporated during the annealing process. The annealed thin films were slightly thinner than the as-grown films. The thicknesses of the *n*- and *p*-type thin films were about 230 nm and 180 nm, respectively.

The EDS results provide the atomic compositions of the as-grown *n*- and *p*-type bismuth telluride and resulting bismuth telluride annealed thin films (Fig. 5). The atomic compositions of the as-grown bismuth telluride thin films and annealed thin films were the same as for bulk material at 473 K, 523 K, 573 K, and 623 K for the *n*-type films and at 473 K, 523 K, and 573 K for the *p*-type films. The atomic composition of antimony is decreased at 623 K for *p*-type bismuth telluride. Similar results were reported in previous work, although the thin films were made by a flash evaporation method.[6] We confirmed that the coaxial-type vacuum arc evaporation method can be applied for fabrication of both *n*-type and *p*-type bismuth telluride thin films.

The XRD patterns of the bismuth telluride thin films are shown in Fig. 6. The diffraction patterns of the thin films clearly reveal the effects of the annealing conditions on the film crystalline structures. The as-grown thin films had weak and broad diffraction peaks, indicating low crystallinity. The diffraction peaks of the *n*-type thin films were strong, and they exhibited preferred orientation along the *c*-axis with higher annealing temperatures. Similar effects of annealing on bismuth telluride films have been reported.[7,17,19] Similar results were obtained for the *p*-type films, although the optimum annealing temperatures were 573 K and 623 K for the *n*-type, and 523 K for the *p*-type films. The thickness of the *p*-type thin film annealed at 623 K was too thin owing to tellurium and antimony evaporation during the annealing process as shown in Fig. 5b.

The thermoelectric properties were measured at room temperature as shown in Fig. 7. The *p*-type thin film annealed at 623 K was too thin to measure its Seebeck coefficient and electrical conductivity. The electrical conductivity was increased upon annealing, although the carrier concentration decreased. The mobility was increased by the annealing process due to crystal grain growth. The highest electrical conductivity of 470/Ω-cm was found for the *n*-type thin film annealed at 523 K. The measured electrical conductivity corresponds to the surface resistance of 93 Ω/□, and it is poorer than the value (22 Ω/□) reported for film prepared by a vacuum arc plasma method.[15] The Seebeck coefficient of the *n*-type thin film was improved by the annealing process. The highest power factor of *n*-type thin film was 10 μW/(cm K^2) when annealed at 573 K. Its electrical conductivity was 417/Ω-cm, and its Seebeck coefficient was -155 μV/K. The electrical conductivity of the *p*-type thin film was improved upon annealing, but decreased with annealing temperatures higher than 573 K. The crystal grains grew in the annealing process, but tellurium and antimony evaporated gradually, as shown in Fig. 5b. Both the carrier mobility and concentration decreased. The highest power factor of *p*-type thin film was 7.1 μW/(cm K^2) when annealed at 523 K. The measured electrical conductivity was 211/Ω-cm, and the Seebeck coefficient was 183 μV/K.

The cross-plane thermal conductivity was measured at room temperature by the differential 3ω method[17,20,21] to evaluate the nondimensional figure of merit of the films. The measured thermal conductivity was in the range of 0.21 W/(m K) to 0.61 W/(m K) for *n*-type and 0.25 W/(m K) to 0.80 W/(m K) for *p*-type. The average thermal conductivity of both *n*- and *p*-type thin films was 0.35 W/(m K) and 0.52 W/(m K), respectively. The measured thermal conductivities were lower than those of other thin films.[17,18] The figure of merit *ZT* was calculated from the electrical conductivity, the Seebeck coefficient, and the average thermal conductivity. The highest *ZT* was 0.86 for *n*-type and 0.41 for *p*-type, for annealing temperature of 573 K and 523 K, respectively.

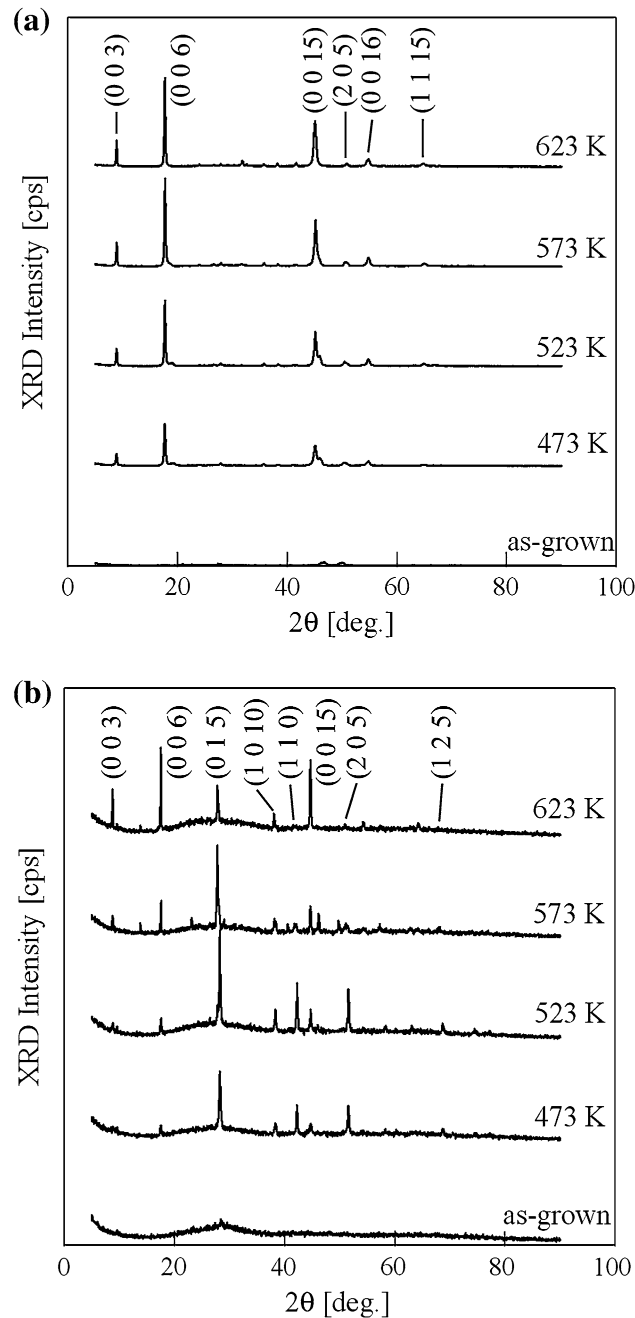

Fig. 6. (a) x-Ray diffraction patterns of *n*-type bismuth telluride thin films. (b) x-Ray diffraction patterns of *p*-type bismuth telluride thin films.

CONCLUSIONS

We proposed fabrication of both *n*- and *p*-type bismuth telluride thin films using a coaxial-type vacuum arc evaporation method. The atomic compositions of the as-grown thin films and several annealed thin films were comparable to that of bulk bismuth telluride. The thermoelectric properties of the bismuth telluride thin films were significantly improved by the annealing process. The crystallization and orientation of the thin films were enhanced along the *c*-axis. The highest *ZT* value was 0.86 and 0.41 for *n*- and *p*-type, for annealing temperature of 573 K and 523 K, respectively. We confirmed that the coaxial-type vacuum arc evaporation method can be applied for fabrication of both *n*-type and *p*-type bismuth telluride thin films, although it is necessary to measure the in-plane thermal conductivity as well as the in-plane electrical properties for further discussion. The thin-film thickness can be easily controlled due to the low deposition rate of the coaxial-type vacuum arc evaporation method. The method can be applied for fabrication of thin films of several nanometer thickness, such as superlattice structures.

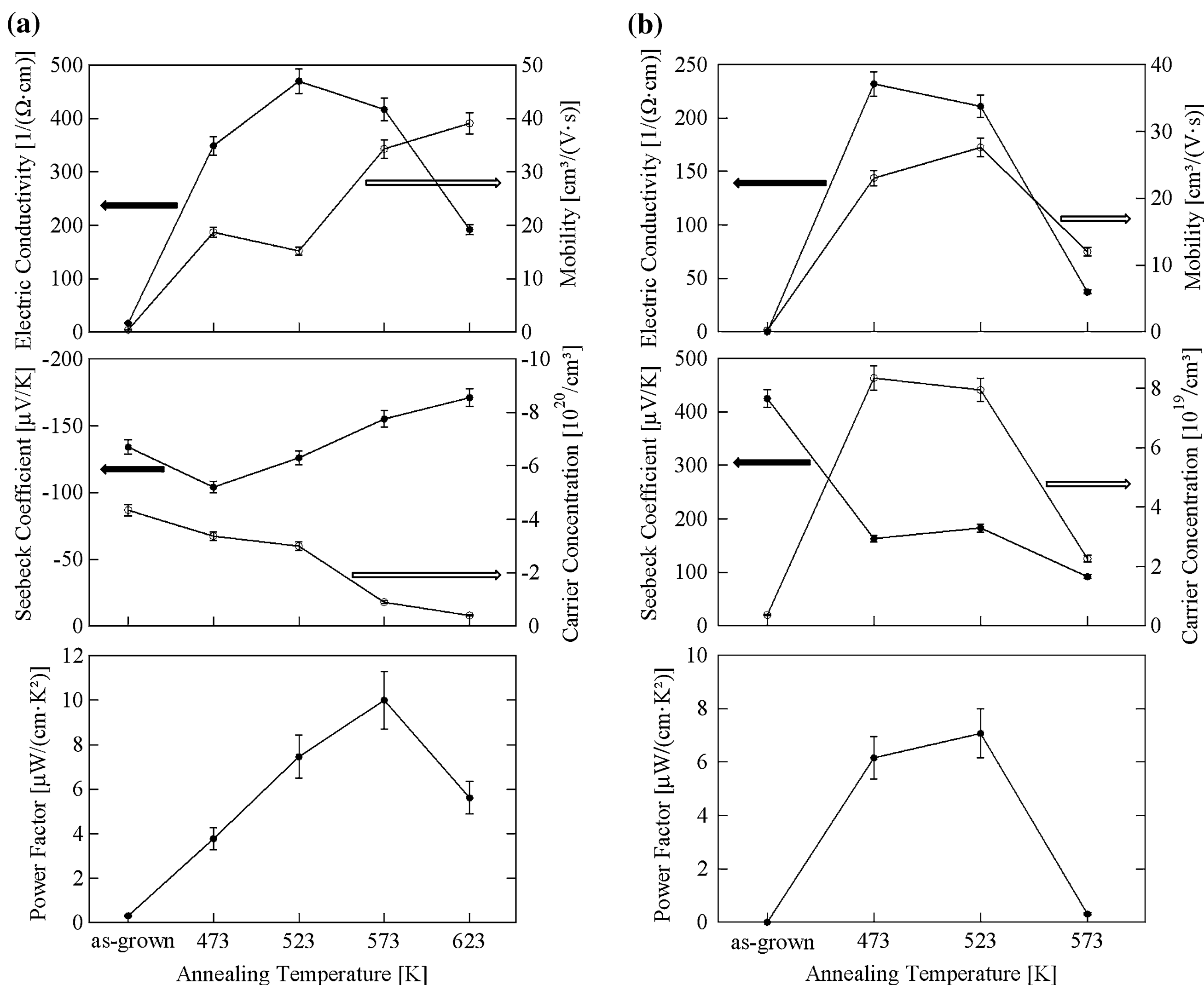

Fig. 7. (a) Annealing temperature dependence of thermoelectric properties of *n*-type Bi_2Te_3 thin films. (b) Annealing temperature dependence of thermoelectric properties of *p*-type Bi_2Te_3 thin films.

REFERENCES

1. W. Zhou, J. Zhu, D. Li, H.H. Hug, F.Y.C. Boey, J. Ma, H. Zhang, and Q. Yan, *Adv. Mater.* 21, 3196 (2009).
2. Y. Lan, A.J. Minnich, G. Chen, and Z. Ren, *Adv. Mater.* 20, 357 (2010).
3. C.J. Vineis, A. Shakouri, A. Majumdar, and M.G. Kanatzidis, *Adv. Mater.* 22, 3970 (2010).
4. J.S. Son, M.K. Choi, M. Han, K. Park, J. Kim, S.J. Lim, M. Oh, Y. Kuk, C. Park, S. Kim, and T. Hyeon, *Nano Lett.* 12, 640 (2012).
5. M. Kashiwagi, S. Hirata, K. Harada, Y. Zheng, M. Yahiro, C. Adachi, and K. Miyazaki, *Appl. Phys. Lett.* 98, 023114 (2011).
6. M. Takashiri, T. Shirakawa, K. Miyazaki, and H. Tsukamoto, *J. Alloys Compd.* 441, 246 (2007).
7. M. Takashiri, K. Miyazaki, and H. Tsukamoto, *Thin Solid Films* 516, 6336 (2008).
8. K. Miyazaki, A. Jaquot, T. Shirakawa, M. Kozasa, and H. Tsukamoto, *Proceedings of the 3rd European Conference on Thermoelectrics*, vol. 116 (2005).
9. H. Böttner, A. Schubert, K.H. Schlereth, D. Eberhard, A. Gavrikov, M. Jägle, G. Kühner, C. Künzel, J. Nurnus, and G. Plescher, *J. Microelectromech. Syst.* 13, 414 (2004).
10. H. Noro, K. Sato, and H. Kagechika, *J. Appl. Phys.* 73, 1252 (1993).
11. R. Venkatasubramanian, T. Colpitts, E. Watko, M. Lamvik, and N. El-Masry, *J. Cryst. Growth* 170, 817 (1997).
12. A. Al Bayaz, A. Giani, M. Al Khalfioui, A. Foucaran, F. Pascal-Delannoy, and A. Boyer, *J. Cryst. Growth* 258, 135 (2003).
13. Y. Yamamoto, Y. Agawa, Y. Hara, S. Amano, A. Chayahara, Y. Horino, and K. Fujii, *International Conference on Ion Implantation Proceeding, 1998*, 2, 1148 (1999).
14. I.V. Gasenkova and E.I. Tochitsky, *Proceedings of XIV International Conference on Thermoelectrics*, 29 (1995).
15. I.V. Gasenkova, *Proceedings of XIV International Conference on Thermoelectrics*, 151 (1997).
16. A. Jacquot, B. Lenoir, A. Dauscher, M. Stölzer, and J. Meusel, *J. Appl. Phys.* 91, 4733 (2002).
17. M. Takashiri, M. Takiishi, S. Tanaka, K. Miyazaki, and H. Tsukamoto, *J. Appl. Phys.* 101, 074301 (2007).
18. M. Takashiri, S. Tanaka, and K. Miyazaki, *Thin Solid Films* 519, 619 (2010).
19. S. Jeon, M. Oh, H. Jeon, S. Hyun, and H. Lee, *Microelectron. Eng.* 88, 541 (2001).
20. S.M. Lee and D.G. Cahill, *J. Appl. Phys.* 81, 2590 (1997).
21. T. Borca-Tasciuc, R. Kumar, and G. Chen, *Rev. Sci. Instrum.* 72, 2139 (2001).